www.czasopisma.pan.pl PAN POLSKA AKADEMIA NAUK www.journals.pan.pl

Arch. Metall. Mater. **65** (2020), 4, 1437-1445

DOI: 10.24425/amm.2020.133711

M. UHRÍČIK[1*], P. PALČEK[1], M. CHALUPOVÁ[1], P. HANUSOVÁ[1], L. KUCHARIKOVÁ[1]

ANALYSIS OF THE PROPERTIES OF EN AC 51200 ALUMINUM ALLOY

The article will be focused on analysis of properties of aluminum alloy for the casting of type Al-Mg. As an experimental material was used aluminum alloy EN AC 51200, supplied in a cast state without a heat treatment. It was produced by the continuous casting method. Experiments deal with microstructural material analysis, fractographic analysis, mechanical and fatigue tests. The microstructure of the testing sample was examined using an optical microscope Neophot 32. Fatigue properties of aluminum alloy was tested by three-point bending cyclic loading. The fracture surface of the testing sample was examined using scanning electron microscopy (SEM), where sample was observed on various stages of the fatigue process, its characteristics and differences of fracture surfaces.

Keywords: aluminum alloy, Al-Mg cast alloy, three-point bending loading, fatigue, fracture surface

1. Introduction

Casting alloys are materials used for the production of shape castings that is aluminum alloy products with complex geometrical shape(s). Casting aluminum alloys are quite widespread and find more and more applications in modern industry [1].

Aluminum alloys are very important engineering materials widely employed in the engineering and structural applications such as automobile parts, aircraft fittings, wire ropes and overhead electrical cables due to its high strength-to-density ratio. Aluminum alloys also undergo fatigue damage in these applications [2].

Aluminum castings are widely used in the automotive industry for several components such as engine blocks and cylinder heads, produced in high volumes, thanks to their favourable combination of low weight, easy machinability, recyclability and low cost [3].

Developments in aluminum alloys and optimization of casting techniques have lead to improved material properties and functional integration which enable aluminum castings to satisfy the new market requirements and have allowed replacing, in many cases, engine components made with heavy cast iron alloys. Nevertheless requirements for new products are becoming more and more challenging for conventional aluminum alloys and their further improvement or the introduction of new alloys are under evaluation [3].

Aluminum alloys intended for use in the automotive industry should possess an appropriate combination of strength and ductility. For example, sheets or profiles are typically formed into final shapes such as body panels or bumper beams by cold deformation. Hence, the bendability of the material is of great importance in fabrication as well as in use, where the ductility is required for optimal energy absorption. Uniaxial tensile testing is often used to determine the mechanical properties of metals. However, this type of test does not always give a good description of the deformation mode experienced by a component. In this case, the three-point bending test is a suitable method for describing the mechanical properties. The bendability is defined as the ratio between the minimum bending radius and the thickness of the test specimen without fracture occurring [4-7]. In 1960, Datsko and Yang [5] came up with a simple relationship between bendability and the reduction in area obtained by tensile testing. This empirical relationship, however, does not include any of the underlying microstructural mechanisms. Several phenomena influence the bendability, e.g., hardening behavior, constituent particles, shear band formation, microstructure, and texture/anisotropy [4].

The fatigue process can in general be divided into two main steps [8,9]: initiation of micro-cracks due to local accumulation of dislocations, high stresses at local points, plastic deformation around inhomogeneous inclusions or other imperfections; crack propagation, which causes permanent damage. The position and

[1] UNIVERSITY OF ŽILINA, FACULTY OF MECHANICAL ENGINEERING, DEPARTMENT OF MATERIALS ENGINEERING, UNIVERZITNÁ 8215/1, 01026 ŽILINA, SLOVAKIA

* Corresponding author: milan.uhricik@fstroj.uniza.sk

mode of fatigue crack initiation depends on the microstructure of the material, the type of the applied stress and geometry of the specimen [8,10]. The crack initiation periods can be very different and cracks can be initiated either on or under surface. Fatigue cracks initiation can be observed in stress concentration points where the resistance area is smaller. The number of cycles, N_f required for fracture can be determined from the number of stress cycles, *Ni*, required for the appearance of the initial crack in the material and the number of stress cycles, *Np* required for a crack to propagate from the initial to the critical crack length, when the final failure can be expected to occur ($N_f = N_i + N_p$) [8].

Castings made of aluminum alloys usually contain various structural discontinuities, which have an essential influence on the strength and fatigue life of these alloys [11].

The aim of this work is to study and analyze properties of aluminum alloy for the casting of type Al-Mg, especially an aluminum alloy EN AC 51200. Experimental measurement is focused on material evaluation and fractographic analysis of fracture surfaces after three-point bending loading.

2. Material and Methods

Commercial aluminum alloy EN AC 51200 was used as an experimental material, supplied by its respective manufacturer in a cast state without heat treatment in the form of ingot (Fig. 1). It was produced by the continuous casting method. The real chemical composition of this alloy was examined by spark emission spectrometer SPECTROMAXx and result is shown in Table 1.

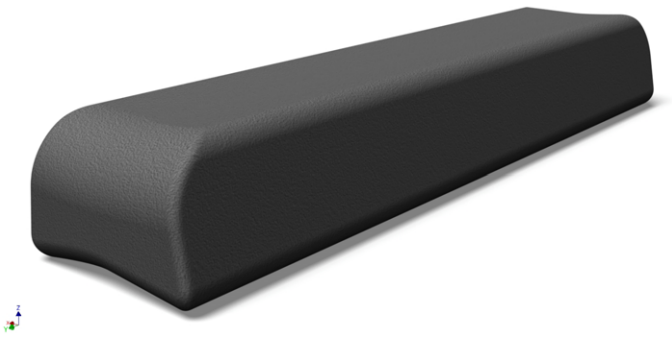

Fig. 1. An ingot of aluminum alloy EN AC 51200

First, the experimental material was subjected to metallographic analysis. The microstructures were studied using an optical microscope Neophot 32 and scanning electron microscope TESCAN Vega II LMU with a Brucker-Quantax analyzer upon deep etching [12,13]. The microstructure of alloy was evaluated in its initial state.

The microstructure of the aluminum alloy EN AC 51200 was significantly dendritic (Fig. 2), which was formed by a matrix of phase α (solid solution of additive elements in aluminum). The intermetallic phase Mg_2Si, phase β (Al_3Mg_2) and other phases formed by the combination of additive elements in the aluminum, for example iron phase ($Al_6(FeMn)$), were found in the interdendritic areas. Figure 3 shows phases in the structure

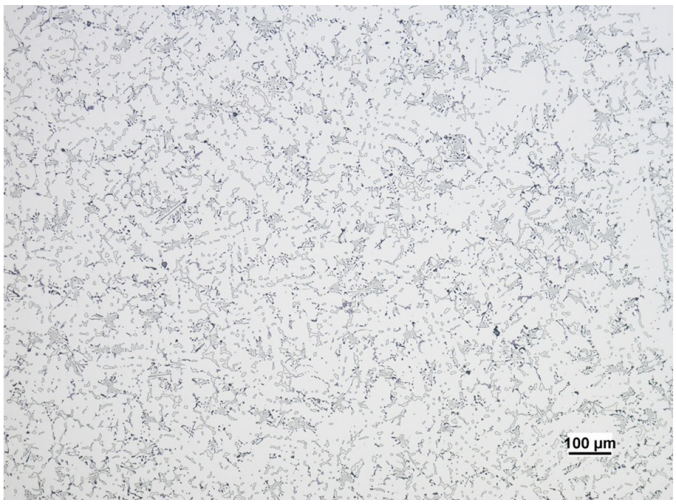

Fig. 2. The microstructure of the aluminum alloy EN AC 51200

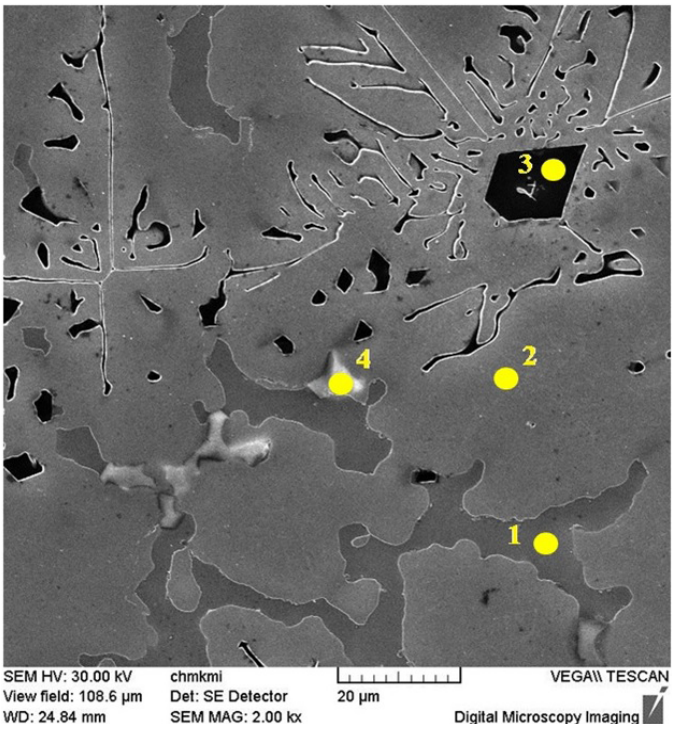

Fig. 3. Identification of phases present in the microstructure of the aluminum alloy EN AC 51200 – point microanalysis of phases

TABLE 1

The chemical composition of aluminum alloy EN AC 51200, in wt. %

	Si	Fe	Cu	Mn	Mg	Cr	Ni	Pb	Al
EN AC 51200	1.3100	0.1020	0.0031	0.4160	10.3210	0.0060	0.0041	0.0270	balance

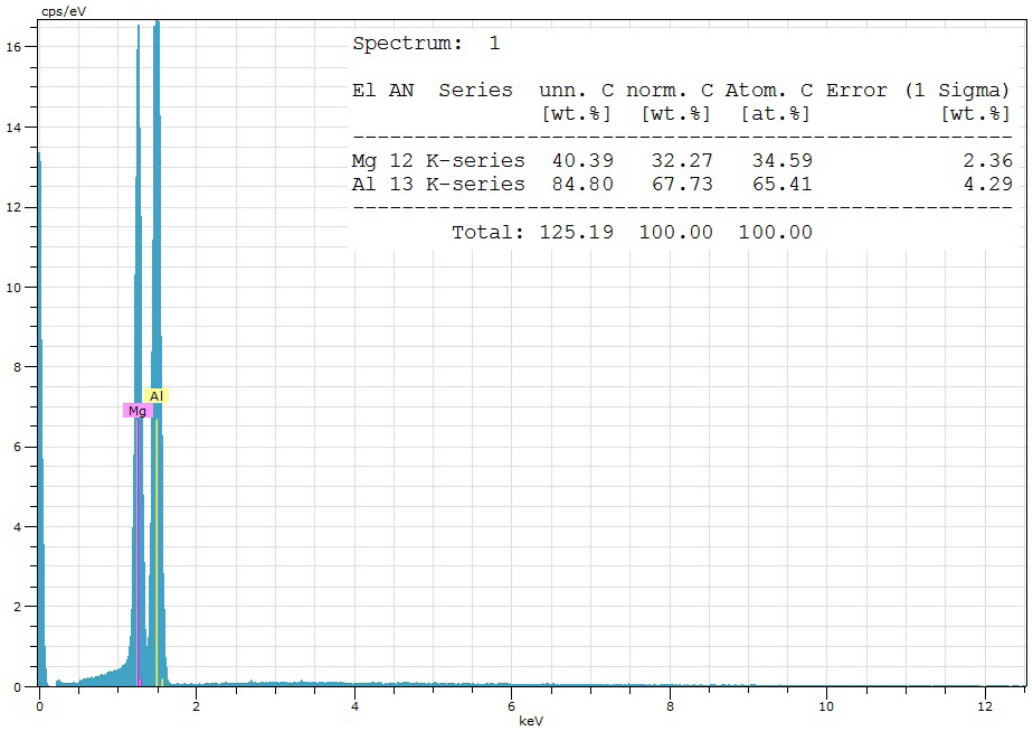

Fig. 4. Spectrum and quantified content of elements in the microstructure for the point 1 from Figure 3 – a confirmation of the presence of Al3Mg2 phase

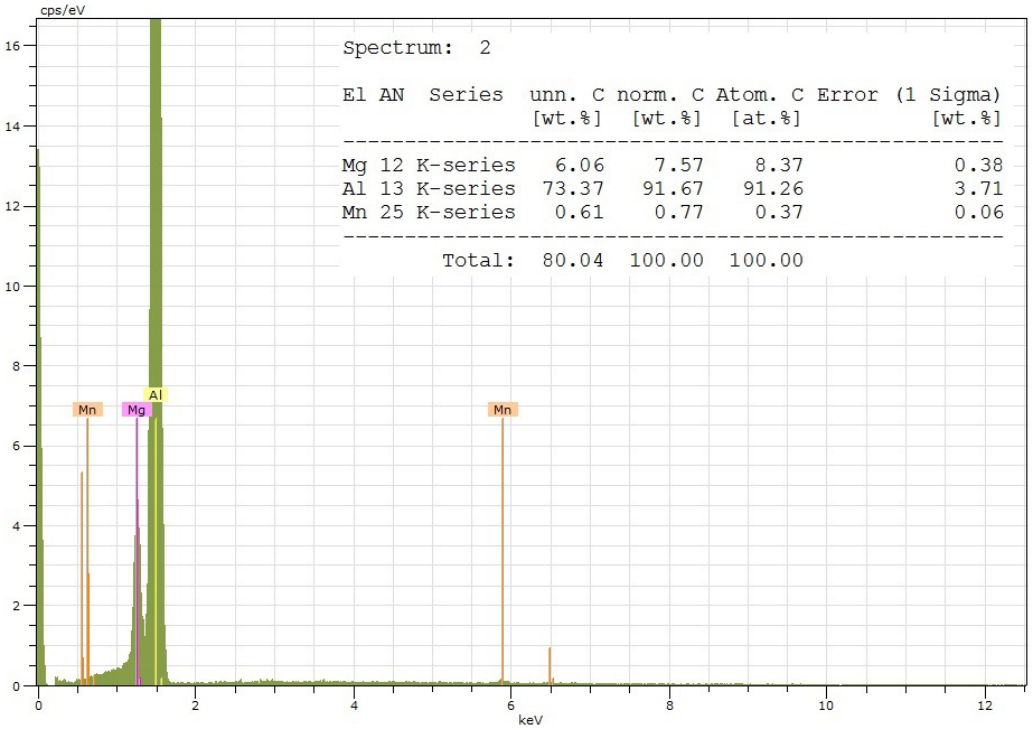

Fig. 5. Spectrum and quantified content of elements in the microstructure for the point 2 from Figure 3 – a matrix

on which the point microanalysis was performed. From Figures 4 to Figures 7, there are spectrums which confirm the presence of individual phases.

A quantitative evaluation was also carried out, which included a percentage assessment of shares of individual phases present in the structure, calculation of the SDAS (Secondary Dendrite Arm Spacing) factor and the grain size. This evaluation was performed on an optical microscope Neophot 32 using a NIKON Coolpix 4500 camera and NIS Elements software.

Percentage assessment of shares of individual phases (Fig. 8) was performed at 1000x magnification and the sample was etched with 0.5% hydrofluoric acid. The phase β had the

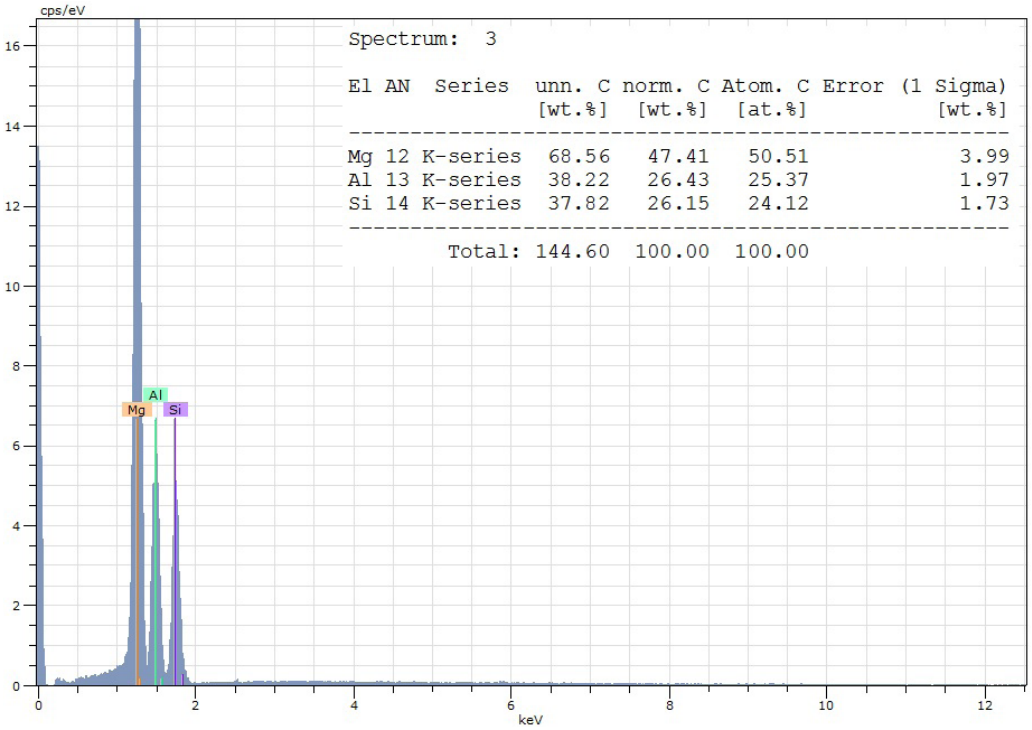

Fig. 6. Spectrum and quantified content of elements in the microstructure for the point 3 from Figure 3 – a confirmation of the presence of Mg2Si phase

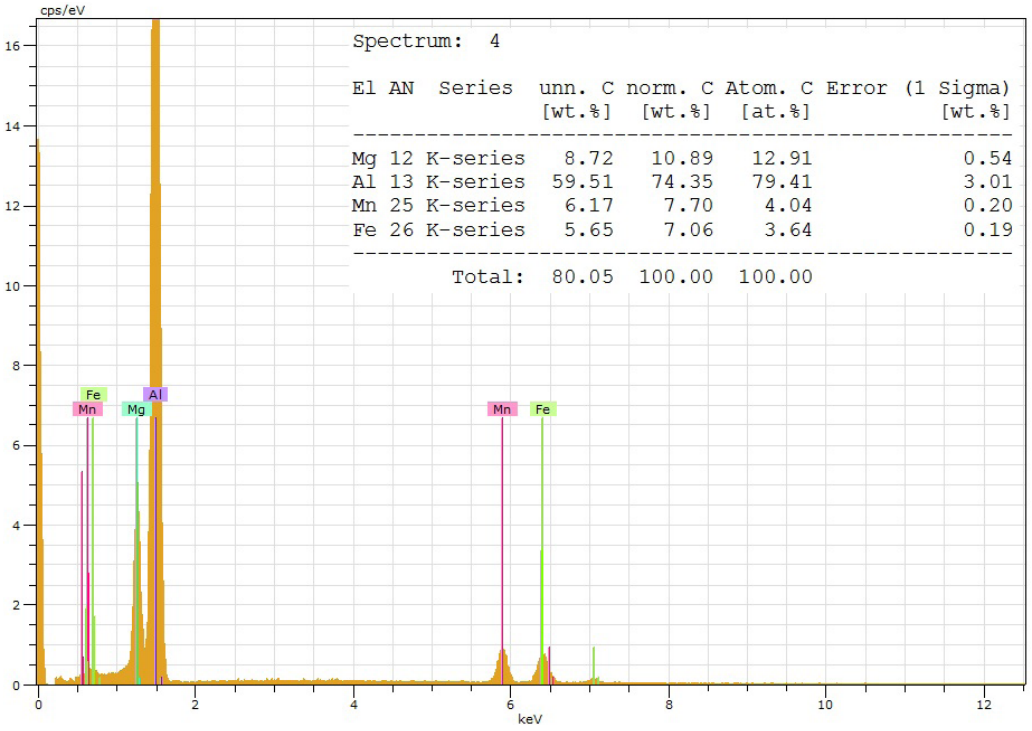

Fig. 7. Spectrum and quantified content of elements in the microstructure for the point 4 from Figure 3 – a confirmation of the presence of Al6(FeMn) phase

largest share in the structure, in the amount of 8.2%. The intermetallic phase Mg_2Si had a share of 6.9% and $Al_6(FeMn)$ phase had a share below the percentage (0.85%). Resulting values of the percentage assessment of shares of individual phases were from twenty measurements.

The SDAS factor was evaluated by a line method, on a matrix at 100× magnification, where the number of perpendicular secondary dendrite arms intersected by a 12 cm long line was counted. The mean value of the SDAS factor was 39 μm from twenty measurements.

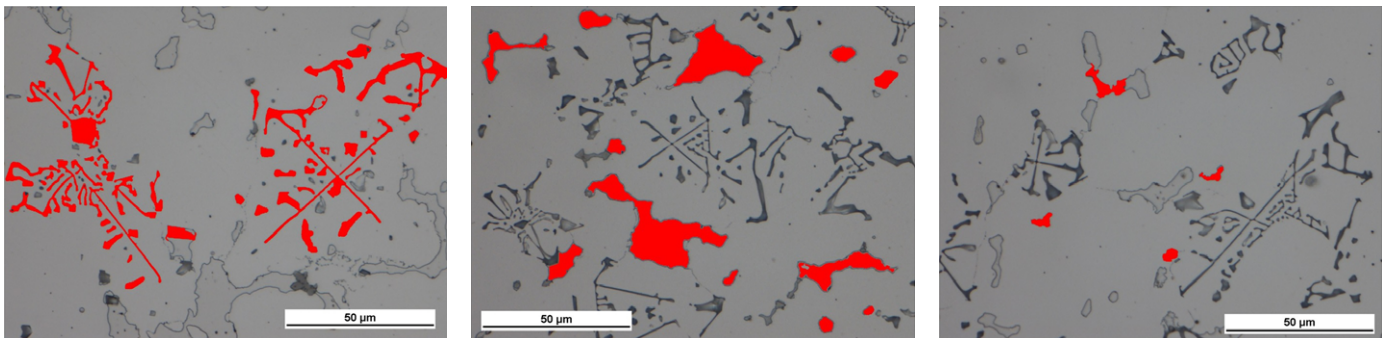

a) a share of Mg_2Si b) a share of Al_3Mg_2 c) a share of $Al_6(FeMn)$

Fig. 8. A measuring of percentage assessment of phases in the alloy EN AC 51200

Grain size evaluation (Fig. 9) was performed at 100× magnification, on a sample after electrolytic etching under polarized light. Grain size was calculated as the area content of individual grains. The resulting value of the grain size is 56455 µm^2 and this is the average value from twenty measurements.

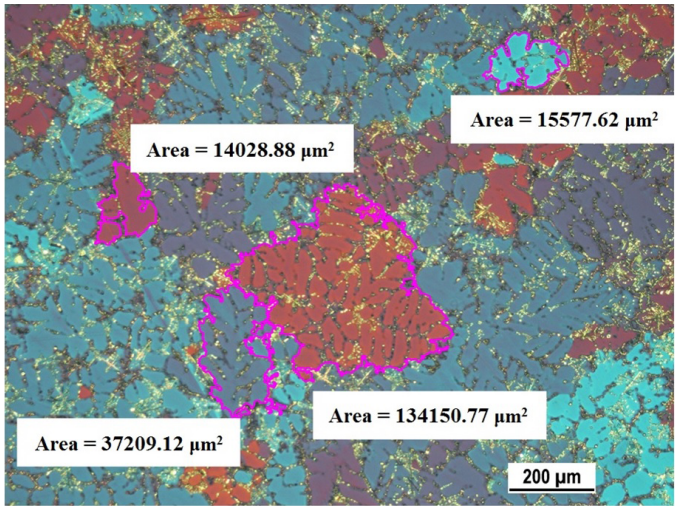

Fig. 9. A grain size measuring of aluminum alloy EN AC 51200

The experimental material of mentioned chemical composition was cut into simple blocky samples with dimensions (w×h×l) 18 mm×10 mm×40 mm (Fig. 10). The three-point bending fatigue test (Fig. 11) has been carried out on testing machine ZWICK/ROELL Amsler 150 HFP 5100 at room temperature 22°C±5°C with static preload force F_{static} = –5.8 kN and dynamic force $F_{dynamic}$ varying from 4.9 kN up to 5.70 kN. The value of 2×10^7 numbers of cycles was set as reference and when specimen has reached this value without break, so called runout, that bending stress was considered as fatigue lifetime limit. The frequency of fatigue tests was approximately f = 120 Hz. The S-N curve was plotted from measured values, which gives relation between stress amplitude σ_o and number of cycles N_f [14,15].

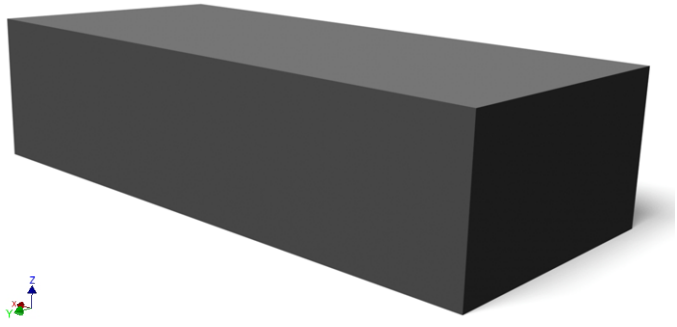

Fig. 10. The specimen for a fatigue test

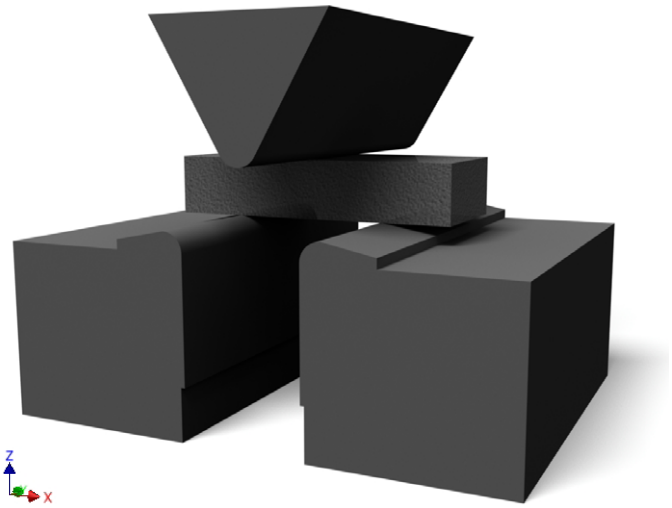

Fig. 11. A display of the three-point bending fatigue test setting

A Vickers hardness test was also performed, according to the STN EN ISO 6507-1 standard on a Zwick/Roell ZHVµ-A test apparatus. As an indenter was an equilateral pyramid (with a square base) made of diamond with a plane angle of 136°, which was pressed into the sample for 10 seconds with a force of 10 kP (HV 0.01) when measuring microhardness and 500 kP (HV 0.5) when measuring total hardness. The resulting average hardness values were from twenty measurements.

The fractography analysis of broken specimens was also done. For fractography analysis scanning electron microscope TESCAN Vega II LMU was used. All fractography analysis was done in order to describe micromechanisms of fatigue crack initiation, fatigue crack propagation and final static fracture of specimens [14,15].

3. Results

For the cyclic three-point bending fatigue test, 18 single block shape samples without notches were used, whose shape is shown in Figure 10. From results of fatigue tests were constructed the S-N curve in semilogarithmic coordinates (Fig. 12). These results were approximated using the Basquin formula (Equation 1) for S-N presentation and approximation, in which the exponents were calculated by the least squares method.

$$\sigma_a = \sigma_f' \times N_f^b \tag{1}$$

where σ_f is a factor of fatigue strength and b is an exponent of lifetime curve.

By the Vickers hardness test, the total hardness of 100 HV 0.5 was measured for the aluminum alloy EN AC 51200. By the microhardness measuring, which is used to determine the hardness of individual phases, the hardness of the α-phase (matrix) 78 HV 0.01 and the hardness of the β-phase (Al_3Mg_2) 230 HV 0.01 were measured. It was not possible to measure the hardness of the Mg_2Si phase and $Al_6(FeMn)$ phase, because these phases are small, respectively fine. As can be seen in Figure 13, during the measurement of the hardness of the Mg_2Si phase, the indentation also intervened in the matrix and thus the measured hardness value was not the hardness of the specific phase, but in this case it was the hardness of the mixture of α-phase and Mg_2Si phase. The same thing happened during the measurement of the hardness of the $Al_6(FeMn)$ phase.

4. Discussion

The microstructure of the investigated material is significantly dendritic and the largest percentage is represented by the α-phase (matrix). According to Boyko [16], approximately

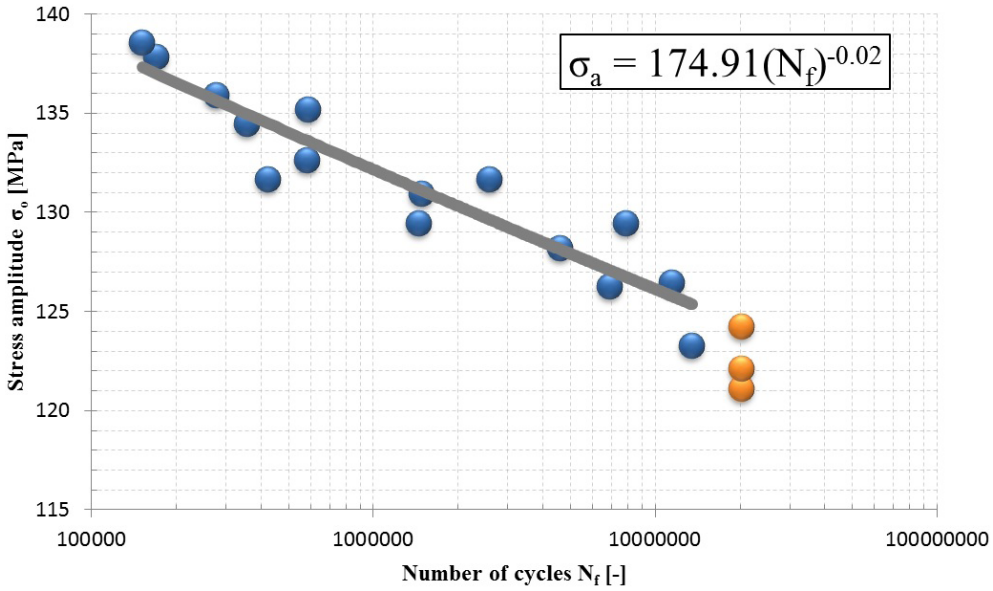

Fig. 12. Results of fatigue tests for EN AC 51200

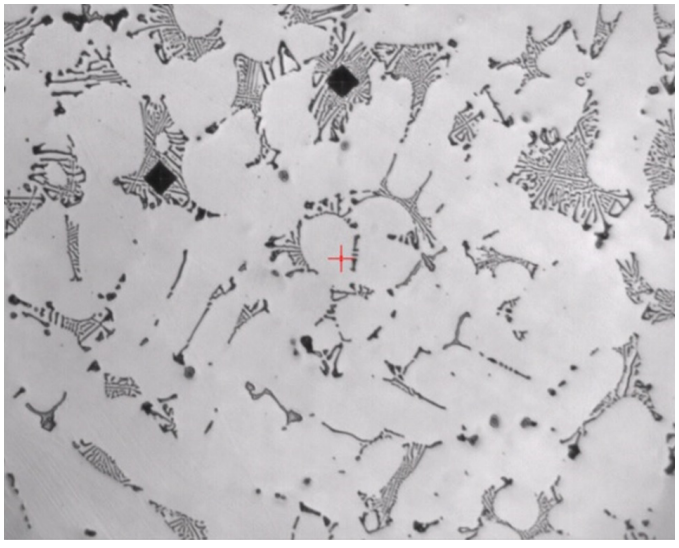

Fig. 13. The measurement of the hardness of the Mg_2Si phase

2±0.4 wt.% of magnesium and 0.38±0.05 wt.% of manganese are present in the solid solution of the α-phase and the balance is aluminum.

Because this type of alloy (Al-Mg) is not described in detail as much as for example an Al-Si type of alloy, details about phases located in the structure were obtained from the publication [17]. It states that the following phases may occur in Al-Mg alloys intended for casting: Mg_2Si, Al_3Mg_2, $Al_6(FeMn)$ and $Al_{18}Mg_3Cr_2$. Results of analyzes show that phases Mg_2Si, Al_3Mg_2 and $Al_6(FeMn)$ were present in the EN AC 51200 alloy, which were precipitated mainly in interdendritic spaces. The presence of the $Al_{18}Mg_3Cr_2$ phase in the structure was not confirmed.

From experimental results and especially from measured S-N curve is possible to see that the fatigue life increases with decreasing stress amplitude. The S-N curve appears to continuously decline as the life extends and orange markers indicate

specimens, which did not fail before the maximum number of cycles, as runout. Fatigue test result stated the limit number of cycles 20000028 at the maximum bending stress $\sigma_{o\max} = 124$ MPa.

In order to examine the fatigue fracture surface, samples were analyzed that were loaded at different maximum stresses and with different fatigue lifetimes.

From the macrofractographic analysis of fracture surfaces, it is possible to determine the site of initiation (nucleation) of the fatigue crack and areas of individual fracture regions (fatigue region and static fracture region). Fatigue crack initiated on the surface of samples (Fig. 14). In the case of samples loaded with higher stress amplitudes, it is possible to observe two initiation sites on the fracture surface. In the case of samples loaded with lower stress amplitudes, it is only one initiation site. The size of the area of stable fatigue crack propagation also depended on the stress amplitude. Fatigue tests determined that the high stress amplitude caused a small fatigue area and a large area of final static rupture. As the stress amplitude decreased, the fatigue area of stable crack propagation increased. Alternatively, it is possible to see the presence of inhomogeneities, especially in cast materials. However, from macrofractographic analysis, it was not possible to determine what was causing the fatigue crack.

From the microfractographic analysis it can be seen that the fatigue area (Fig. 15) is characterized by transcrystalline fatigue failure of the α-phase. Intermetallic phases were an interphase failure in this area, at the matrix-phase interface. In all samples it was possible to observe typical fatigue features in this area, striations (Fig. 16).

In the region of a static fracture (Fig. 17), it can be said that a transcrystalline ductile fracture with dimple morphology and with plastically deformed ridges is typical for a rupture of α-phase. Intermetallic phases were also an interphase failure in this region.

5. Conclusion

The article provides information about the material and fractures of aluminum alloy EN AC 51200 in the mode of three-point bending. An S-N curve was constructed from measured values and it is clear from it that the fatigue life increases with decreasing stress amplitude. The S-N curve appears to continuously decline as the life extends and the limit number of cycles 2.10^7 (20000028) was reach at maximum bending stress $\sigma_{o\max} = 124$ MPa.

From macrofractographic and especially also from microfractographic analysis of fracture surfaces, it was not possible to determine what the fatigue crack initiated. It is assumed, that it is caused either by notches after machining or by intermetallic phases which act in the alloy as stress concentrators on which a fatigue crack could initiate.

Acknowledgement

This work has been supported by Scientific Grant Agency of Ministry of Slovak republic and Slovak Academy of Science, N°013ŽU-4/2019 (KEGA), N°016ŽU-4/2020 (KEGA) and N°1/0398/19 (VEGA).

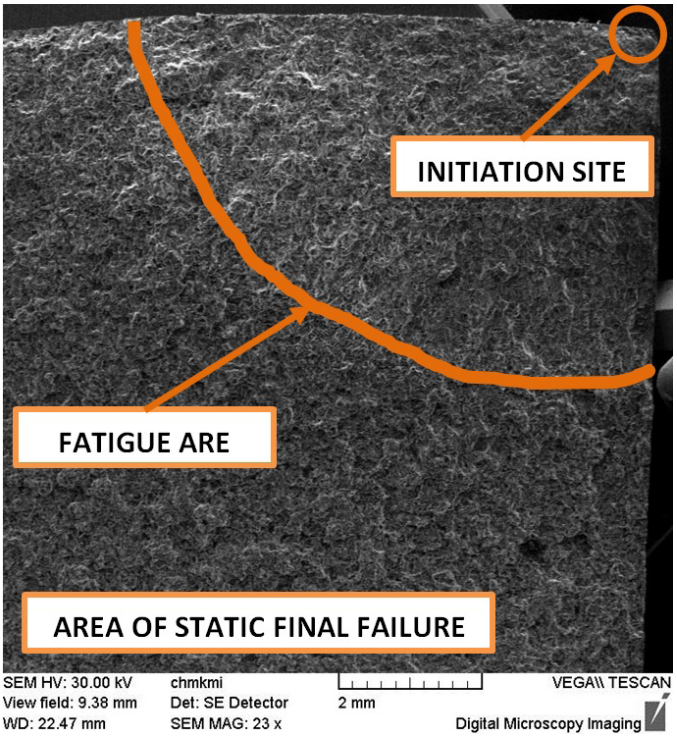

a) Initiation site at lower cyclic loading, one initiation point

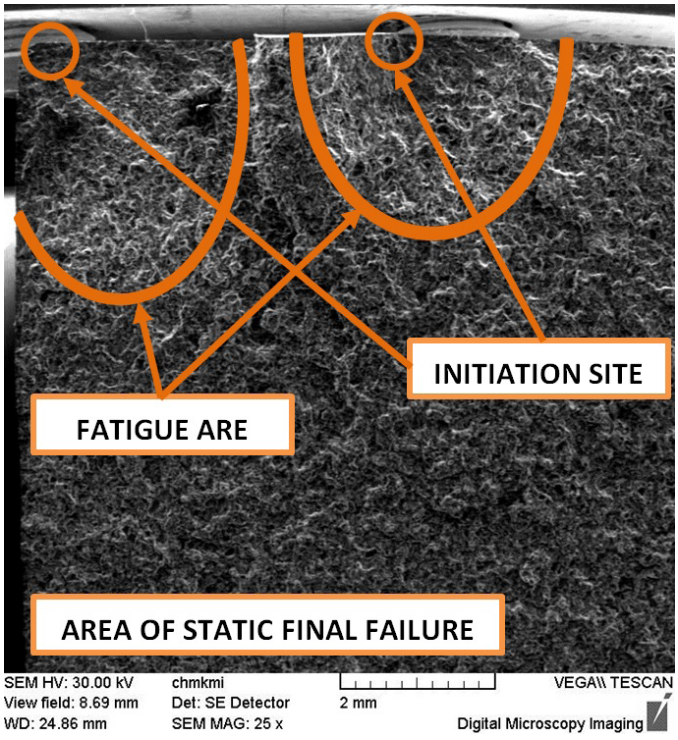

b) Initiation site at higher cyclic loading, two initiation points

Fig. 14. Fractography surface of aluminum alloy EN EC 51200 after three-point bending fatigue test, SEM

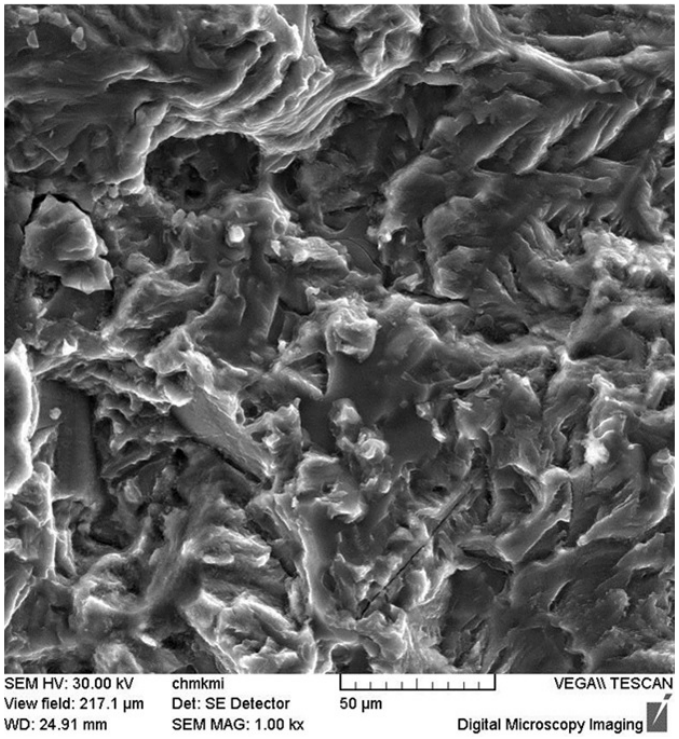

a) Fatigue area at lower cyclic loading

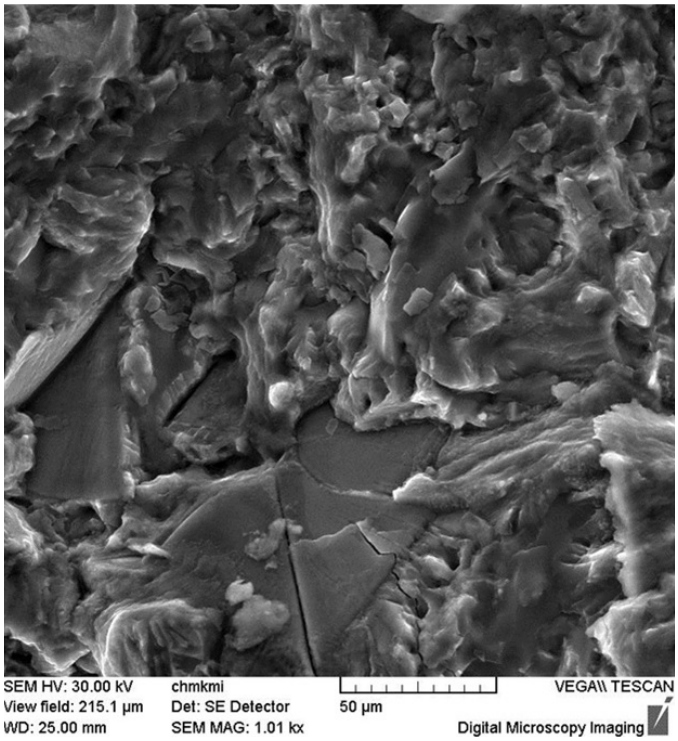

b) Fatigue area at higher cyclic loading

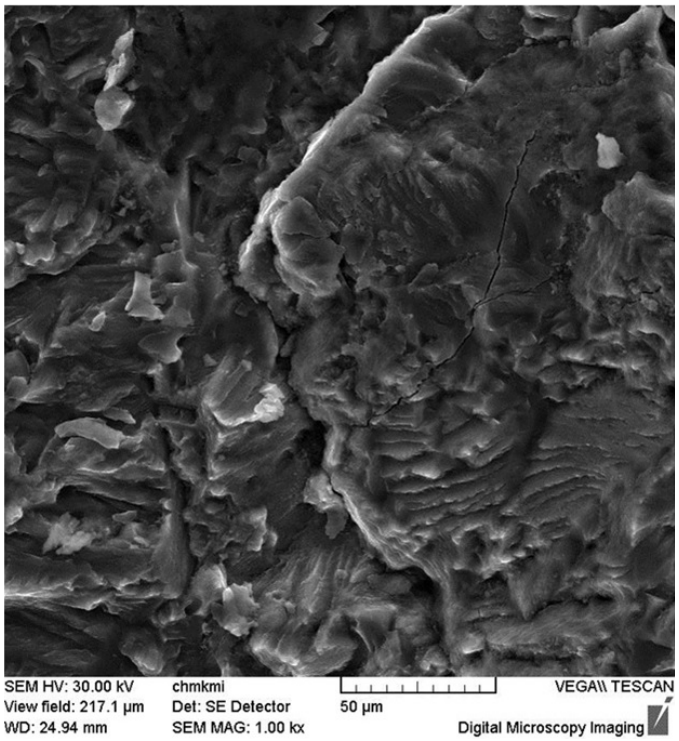

c) Fatigue area at lower cyclic loading – another place

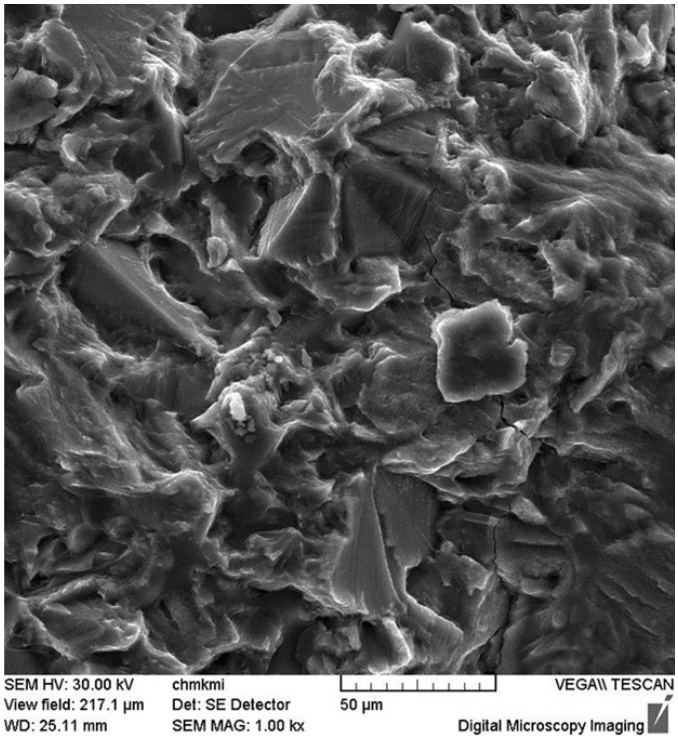

d) Fatigue area at higher cyclic loading – another place

Fig. 15. Fractography surface of aluminum alloy EN EC 51200 after three-point bending fatigue test, SEM

REFERENCES

[1] M.V. Glazoff, V.S. Zolotorevsky, N.A. Belov, Casting Aluminum Alloys, Elsevier, The Netherlands (2007).

[2] R. Sadeler, S. Atasoy, H. Altun, Metallic Materials **47** (2), 95-100 (2009).

[3] R. Molina, P. Amalberto, M. Rosso, Metallurgical Science and Technology **29** (1), 5-15 (2011).

[4] I. Westermann, K.E. Snilsberg, Z. Sharifi, O.S. Hopperstad, K. Marthinsen, B. Holmedal, Metallurgical and Materials Transactions A. **42**, 3386-3398 (2011). https://doi.org/10.1007/s11661-011-0768-y

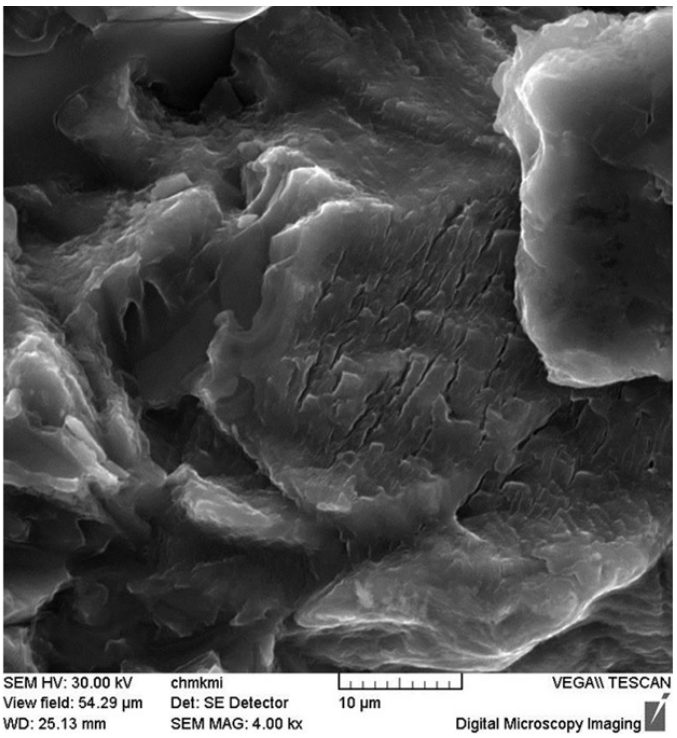

Fig. 16. Fractography surface of aluminum alloy EN EC 51200 after three-point bending fatigue test, SEM – typical fatigue features in fatigue area – striations

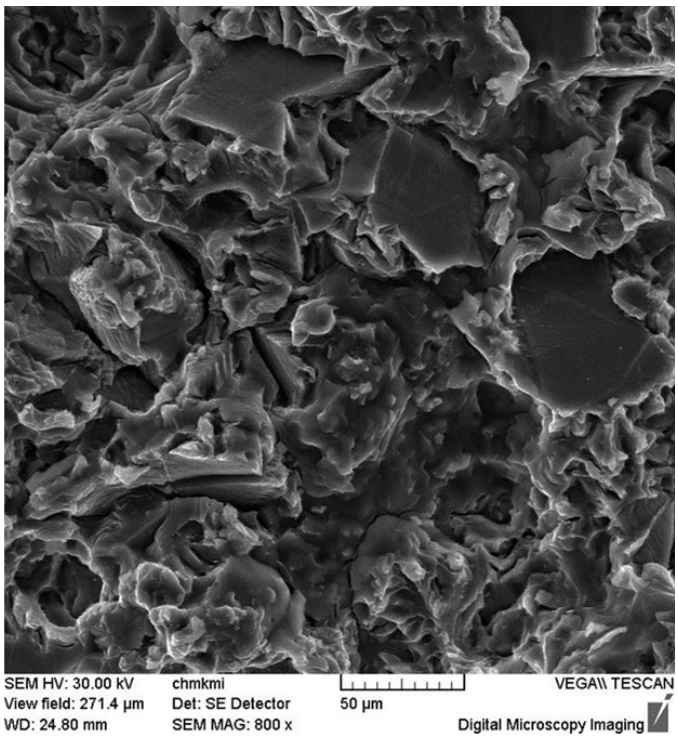

Fig. 17. Fractography surface of aluminum alloy EN EC 51200 after three-point bending fatigue test, SEM – static part of fatigue fracture

[5] J. Datsko, C.T. Yang, J. Eng. Ind. **82** (4), 309-313 (1960) https://doi.org/10.1115/1.3664236

[6] Ch. Wang, G. Kinzel, T. Altan, Journal of Materials Processing Technology **39** (3-4), 279-304 (1993). https://doi.org/10.1016/0924-0136(93)90164-2

[7] C. Iacono, J. Sinke, R. Benedictus, Journal of Manufacturing Science and Engineering **132** (2), 1-9 (2010). https://doi.org/10.1115/1.4000960

[8] C. Vidal, R. Baptista, V. Infante, Matec Web of Conferences **165** (3/4), (2018). https://doi.org/10.1051/matecconf/201816521008

[9] G. Fajdiga, M. Sraml, Engineering Fracture Mechanics **29**, 1320-1335 (2009). https://doi.org/10.1016/j.engfracmech.2009.02.005

[10] W. Cheng, H.S. Cheng, T. Mura, L.M. Keer, Journal of Tribology **116** (1), 2-8 (1994). https://doi.org/10.1115/1.2927042

[11] J. Zych, J. Piekło, M. Maj, A. Garbacz-Klempka, M. Piękoś, Archives of Metallurgy and Materials **64** (2), 765-771 (2019). https://doi.org/10.24425/amm.2019.127611

[12] L. Hurtalová, E. Tillová, M. Chalupová, J. Belan, A. Vaško, Manufacturing Technology **14** (3), 326-333 (2014).

[13] J. Belan, L. Kuchariková, A. Vaško, E. Tillová, Manufacturing Technology **16** (5), 865-870 (2016).

[14] J. Belan, A. Vaško, L. Kuchariková, E. Tillová, Matec Web of Conferences **157** (4), (2018). https://doi.org/10.1051/matecconf/201815707001

[15] J. Belan, L. Kuchariková, E. Tillová, M. C halupová, Advances in Materials Science and Engineering **2019**, 1-11 (2019). https://doi.org/10.1155/2019/2842416

[16] V. Boyko, T. Link, K. Mykhalenkov, Metallurgy and Foundry Engineering **40** (3), 111-124 (2014). https://doi.org/10.7494/mafe.2014.40.3.111

[17] G.F. Vander Voort (Ed.), ASM Handbook: Metallography and Microstructures, USA: ASM International (2004).